



Cite this: *Analyst*, 2019, **144**, 421

Received 15th November 2018,
 Accepted 12th December 2018

DOI: 10.1039/c8an02206b

rsc.li/analyst

Metal coordination-functionalized Au–Ag bimetal SERS nanoprobe for sensitive detection of glutathione†

Pan Li,^a Meihong Ge,^{a,b} Liangbao Yang  ^{*a,b} and Jinhui Liu^a

We demonstrated a surface-enhanced Raman spectroscopy (SERS) nanoprobe, neocuproine-Cu (Nc-Cu^{II})-functionalized Au–Ag “nanobowls” (Au–Ag NBs/Nc-Cu^{II}), for detection of glutathione (GSH). Detection was accomplished with alternation of SERS spectra from Nc-Cu^{II} into Nc-Cu^I resulting from the reaction of GSH with Nc-Cu^{II} on Au–Ag NBs. This nanoprobe exhibited high selectivity and sensitivity (μM) towards GSH.

On the basis of important oxidation–reduction reactions or permeation enhancement of drug molecules, the low-molecular-weight thiol compounds play important parts in many biological and pharmacological reactions.^{1,2} Among the low-molecular-weight thiol compounds, glutathione (GSH, γ-L-glutamyl-L-cysteinyl-glycine) is the most abundant endogenous thiol compound, with concentrations ranging from 0.5 mM to ~10 mM *in vivo*.³ Moreover, GSH with the reduced form (95%) is closely related with various diseases, including Parkinson’s disease, cystic fibrosis, acquired immune deficiency syndrome (AIDS), human immunodeficiency virus (HIV) infection and cancer.^{4–7} In particular, a high concentration of GSH interferes with the efficacy of anticancer therapy.⁸ Consequently, credible detection or monitoring of GSH using a simple and efficient analytical strategy is important for various biochemical and medical applications. Over the past decades, several efforts have been made to establish and develop analytical methods for sensitive detection of GSH: fluorescence spectrometry,^{9,10} liquid chromatography-mass spectroscopy¹¹ and electrochemical analyses.¹² These classical techniques are reliable for detecting GSH, but they suffer from the disadvantages of complicated sample preparation and expensive instruments.

A fluorescent method can provide sensitive and selective detection of GSH, but it undergoes photo-bleaching and photo-degradation.

Over the past over 40 years, surface-enhanced Raman spectroscopy (SERS) has been a powerful and important analytical method in material science and biomedical studies.^{13–15} More importantly, SERS demonstrates particular advantages in bio-analysis owing to the “fingerprint” information of molecular Raman spectra and high sensitivity, even down to the level of a single molecule from plasmonic nanostructures.¹⁶ Conversely, the bandwidth of SERS peaks is usually very narrow, which is beneficial for multiplex detection.^{17–19} Thus, SERS should provide high sensitivity for GSH detection in complex specimens. Sánchez-Illana and co-workers reported use of Ag colloids as SERS substrates for highly selective signal enhancement for GSH combined with a point-of-care (POC) device.²⁰ However, GSH has low polarization and low Raman cross-section, so direct or label-free SERS detection of GSH molecules is not sensitive.²¹

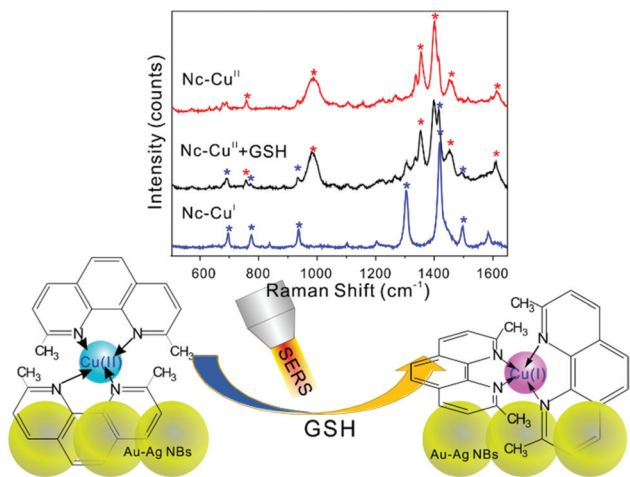
Yang *et al.* developed a (pyridyldithio)ethylamine (PDEA)-modified Ag NPs@Si substrate for sensitive detection of GSH using SERS based on thiol-disulfide exchange sensing.²² Liu *et al.* used 2-nitrobenzoic acid-modified Ag NPs/Si as a Raman-reactive reporting agent for GSH determination based on an enzymatic recycling method.²³ For GSH, an indirect analytical method is convenient, but it is difficult to obtain credible detection based only on alteration of probes in SERS intensity.

In this work, based on the classical redox pair of GSH/GSSG, we developed a SERS nanoprobe composed of Au–Ag “nanobowls” (Au–Ag NBs) and a cupric-neocuproine probe (Nc-Cu^{II}) to determine GSH (Scheme 1). First, Au–Ag NBs acted as SERS substrates for amplifying Raman signals. Meanwhile, Nc-Cu^{II}, possessing high SERS responsiveness, was conjugated on the surface of Au–Ag NBs to fabricate the nanoprobe Au–Ag NPs/Nc-Cu^{II}. We hypothesized that, in the presence of GSH, the Nc-Cu^{II} on Au–Ag NBs would be transformed into an Nc-Cu^I configuration, accompanied with alteration of SERS

^aInstitute of Intelligent Machines, Chinese Academy of Sciences, Anhui, Hefei 230031, China. E-mail: lbyang@iim.ac.cn

^bDepartment of Chemistry, University of Science & Technology of China, Hefei 230026, Anhui, China

† Electronic supplementary information (ESI) available: Experimental section, stability of nanoprobe, UV-vis spectra of nanoprobe. See DOI: 10.1039/c8an02206b



Scheme 1 SERS sensing mechanism of GSH with a nanoprobe Au–Ag NBs/Nc-Cu^{II} (schematic).

spectra. Thus, an Au–Ag NBs/Nc-Cu^{II} nanoprobe could enable monitoring of endogenous GSH.

Excellent SERS substrates require a strong surface plasmon resonance (SPR) effect and high chemical stability. In comparison with an Au nanostructure with high stability, an Ag nanostructure can provide high enhancement, but it is easily oxidized to affect stability. In this report, Au–Ag bimetallic nanostructures were synthesized through a replacement reaction.²⁴ A typical transmission electron microscopy (TEM) image of an Au–Ag bimetal with an average diameter of 80 nm demonstrated a nanobowl nanostructure which could provide large active sites for SERS enhancement (Fig. 1A). SPR from the UV-vis spectra of Au–Ag NBs was observed in the range 400–600 nm with a maximum adsorption peak at 453 nm (Fig. 1B). This is efficient for Raman enhancement at 532 nm

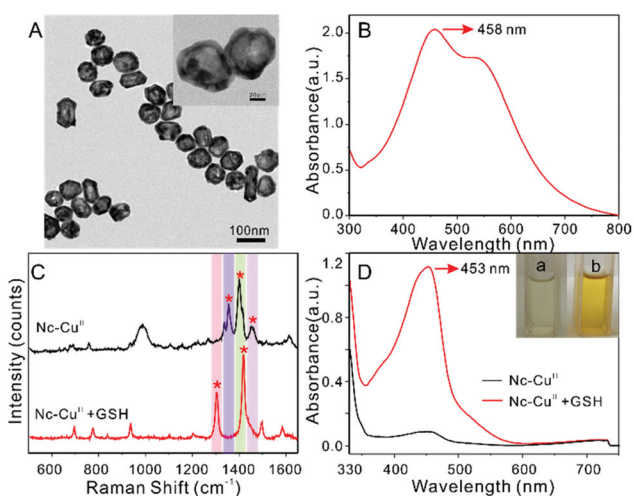


Fig. 1 TEM images (A) and UV-vis spectrum (B) of bimetallic Au–Ag NBs. Alteration of SERS spectra (C), UV-vis spectra (D) and the corresponding optical image (insert in (D)) of Nc-Cu^{II} in the absence and presence of GSH.

excitation because of the matched SPR in aggregated or assembled states.²⁵ GSH is a small-molecule peptide consisting of three amino-acid residues (glutamate, cysteine and glycine). Because of the small Raman cross-section of amino-acid residues, the GSH molecule has a weak SERS response (Fig. S1†), so direct GSH analyses with Au–Ag NBs are difficult. Also, background signals of the substrate may arise from the nitrate and citrate during the growth of Ag NPs and replacement reaction of HAuCl₄, which have a low impact on further SERS detection.

As mentioned above, direct detection of GSH using the SERS method is difficult because GSH has small Raman scattering. Consequently, we proposed the Raman probe Nc-Cu^{II} to indirectly realize sensitive detection of GSH. Although metal ions such as Cu^{II}/Cu^I can also take part in redox reactions, whether GSH is interacting with a free ion or binding to metal ion is unclear. The low-valence metal centre Cu(I) can chelate heteroaromatic ligands to form important compounds with high stability.²⁶ Hence, on the basis of redox reactions, Nc-Cu^{II} is reduced to the Nc-Cu^I chelate in the presence of GSH, and then provides indirect SERS for GSH. With the Nc-Cu^{II} modifying Au–Ag NBs, the SERS property of nanoprobe and GSH responsiveness were studied. As illustrated in Fig. 1C, a clear and abundant SERS spectrum (black line) could be observed for the Au–Ag NBs/Nc-Cu^{II} nanoprobe washed with ultrapure water, thereby indicating functionalization of Nc-Cu^{II} molecules on Au–Ag NBs. When GSH was introduced into Au–Ag NBs/Nc-Cu^{II}, the SERS spectrum changed significantly (red line in Fig. 1C). Specifically, disappearance of bands at 1400 and 1352 cm⁻¹ was accompanied by the appearance of bands at 1415 and 1350 cm⁻¹. These changes in spectra revealed the transformation of Nc-Cu^{II} on Au–Ag NBs into Nc-Cu^I chelates resulting from the reaction of GSH with Nc-Cu^{II}, which possibly caused the configuration of the coordination. Moreover, UV-vis spectroscopy of the Nc-Cu^{II} solution in the presence of GSH also confirmed that the Au–Ag NBs/Nc-Cu^{II} nanoprobe was specifically responsive to the reductive reaction. As indicated in Fig. 1D, upon addition of GSH into Nc-Cu^{II} solution, a new peak at 453 nm appeared along with a colour change, from light-yellow to saffron-yellow, of the solution. A series of UV-vis spectra with alteration of GSH concentration is shown in Fig. S2.† The colour of the Nc-Cu^{II} solution changed gradually from light-yellow to deep-yellow with increasing GSH concentration (Fig. S2A†). Also, the maximum adsorption at 453 nm increased because of the reductive reaction of the Nc-Cu^{II} probe into the highly coloured Nc-Cu^I chelate (Fig. S2B and C†). To evaluate the stability of the nanoprobe Au–Ag NBs/Nc-Cu^{II}, different concentrations of GSH were added to Au–Ag NBs/Nc-Cu^{II} (Fig. S3†). As high-concentration GSH was added to colloids, the colour of colloids changed rapidly to gray-black from khaki, indicating the poor stability of colloids. As decreasing concentrations of GSH were added to Au–Ag/Nc-Cu^{II} colloids, the colour of colloids changed slightly, which could elicit reliable SERS measurements.

Accurate detection of GSH is clinically important because various diseases are associated with GSH. Though GSH has a

small Raman cross-section, a nanoprobe of Au–Ag NBS/Nc-Cu^{II} with rich SERS characteristics could respond indirectly to GSH based on a redox reaction. An “ideal” Raman label for sensing applications should induce abundant Raman spectra and stable responses and have stable properties. Thus, the stability of Raman labels was evaluated (Fig. S4†). The alteration in SERS spectra of the label was minimal, and demonstrated the stability of the Nc-Cu^{II} complex on Au–Ag NBS. As shown in Fig. 2A, with an increasing concentration of GSH, the Raman intensity at 758, 1356, 1400, 1450 and 1604 cm⁻¹ decreases, whereas it increased at 693, 774, 1305, 1415 and 1579 cm⁻¹, which demonstrated a redox reaction along with alteration of the complex probe from Nc-Cu^{II} to Nc-Cu^I. For the labile metal centre Cu(I), phenanthroline derivatives with methyl groups in 2 and 9 positions are highly selective for Cu(I).²⁷ Thus, the Nc-Cu^{II} nanoprobe could be transferred into Nc-Cu^I on Au–Ag NBS substrates to reveal, indirectly, the response of GSH. To

demonstrate further the alteration of characteristic bands, the corresponding peak areas are shown in Fig. 2B. With an increasing concentration of GSH, the peak area of 1415 cm⁻¹ increased (black point) and that at 1400 cm⁻¹ decreased (red point).

More importantly, if the GSH concentration was >100 μM or <0.75 μM, the alteration in peak area of 1400 or 1415 cm⁻¹ plateaued gradually. This finding suggested that the nanoprobe was contributing to GSH at 0.75–100 μM, thereby fulfilling the requirements for evaluating the GSH level in different biofluids.

Most biological events occur at pH 4–9. Thus, stability tests of the nanoprobe in the presence and absence of GSH at different pH conditions are necessary. As indicated in Fig. S5,† with increasing pH, the Raman intensity of the nanoprobe decreased. The most characteristic peaks of the nanoprobe were difficult to distinguish at a pH greater than 8–9. Nc-Cu^{II} may have been hydrolysed partially to precipitate under high pH conditions, leading to lower Raman intensity or weaker Raman features. Moreover, the stability of the nanoprobe was also evaluated in the presence of GSH, and the corresponding spectra at different pH values are shown in Fig. S6.† Similarly, owing to hydrolysis of the nanoprobe, Nc-Cu^{II} could be transferred into Nc-Cu^I within a lower pH range, from 4 to 7. That is, the probe Au–Ag NBS/Nc-Cu^{II} demonstrated high stability against pH change from 4 to 7, which is suitable for SERS detection of bio-fluids containing GSH. More importantly, considering the possible redox reaction between Nc-Cu^{II} and Au–Ag colloids, or between the target molecule GSH and colloids, a longer incubation time should be avoided and dry nanostructure film-based SERS detection should be undertaken.

The organic molecules of an intracellular system or biological fluids, especially amino acids and proteins with sulfhydryl groups or organic molecules with reducing capacity, can interfere in the detection of GSH. Hence, the selectivity of the nanoprobe was investigated with different types of interference. As demonstrated in Fig. 3A–C, the Nc ligand can chelate the metal ions of an intracellular system or biological fluids, including Cu^{II}, Na^I, K^I, Fe^{II}, Mg^{II} and Ca^{II}, and then indicate SERS features, whereas only the SERS spectra of nanoprobe Nc-Cu^{II} changed in response to GSH. In comparison with the Fe^{II}-complex, phenanthroline derivatives with moderately bulky substituents, such as methyl groups in 2 and 9 positions, are highly selective for Cu(I) over Fe(II).^{26,28} Therefore, Nc-Cu^{II} complexes could act as SERS nanoprobe for detection of GSH. For the other possible interferences shown in Fig. 3D–F, most were negligible, except those of Cys and ascorbic acid (AA). The free SH group in Cys molecules or AA with reducing capacity may take part in the redox reaction from Nc-Cu^{II} to Nc-Cu^I, resulting in a slight alteration of signals. Both the GSH and interferences were added onto the nanoprobe Au–Ag NBS/Nc-Cu^{II}, so the nanoprobe Nc-Cu^{II} was transferred to Nc-Cu^I, thereby demonstrating high response towards GSH over that of Cys and AA. To show directly the response of GSH, Cys and AA towards the nanoprobe, UV-vis spectra were collected and summarized. As shown in Fig. S7 and 8,† the discrepancies from inspection of linear calibration curves of GSH in AA (Fig. S7†) and AA in GSH (Fig. S8†) showed that the nanoprobe Nc-Cu^{II}

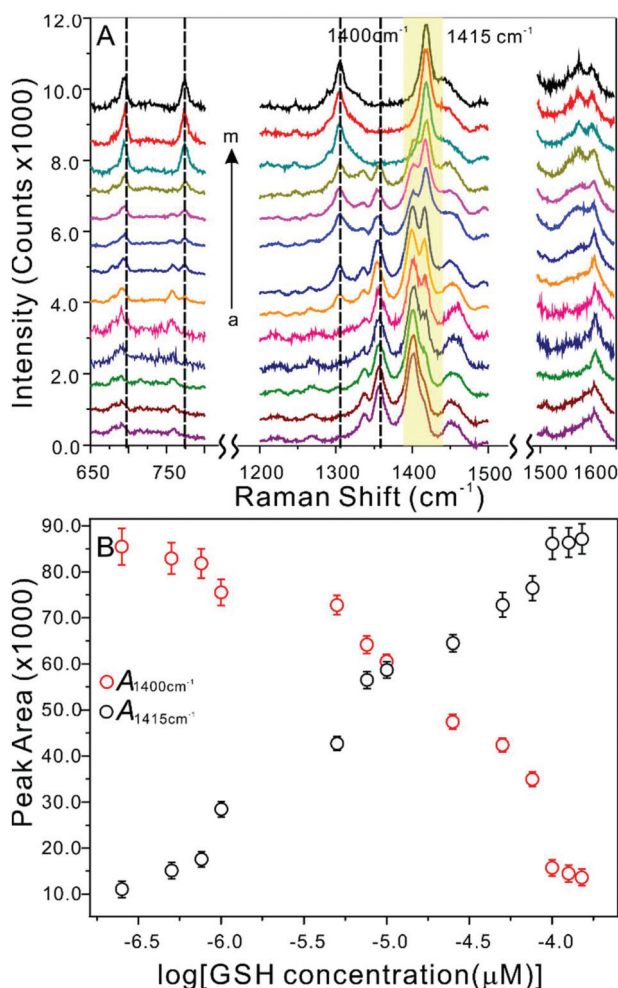


Fig. 2 (A) SERS spectra of nanoprobe Au–Ag NBS/Nc-Cu^{II} (1 μM) in the presence of GSH (from a to m: 0.25, 0.5, 0.75, 1.0, 5.0, 7.5, 10, 25, 50, 75, 100, 250 and 500 μM, respectively). (B) Plots of peak area versus logarithmic GSH concentration based on 1400 and 1415 cm⁻¹. Each data point represents the average value from three independent SERS spectra. Error bars equal the standard deviations.

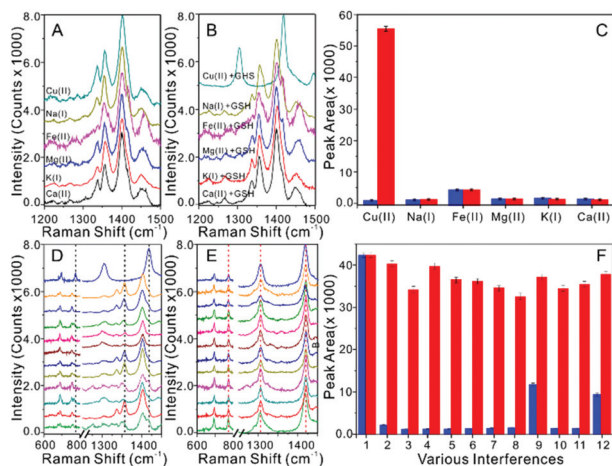


Fig. 3 SERS spectra of Nc ligand and different metal ions (A) in the absence and (B) presence of GSH. (C) Peak area at 1415 cm^{-1} based on the spectra in (A) and (B). SERS spectra of nanoprobe (D) in the presence of various biologically relevant analytes and (E) in the presence of GSH and corresponding various biologically relevant analytes (Nc-Cu^{II}/1–12: GSH, L-cys, serotonin, L- α -ala, L-glu, Glu, D-asp, L-lys, ascorbic acid, DL-leu, glucose and Cys). (F) The peak area at 1415 cm^{-1} based on the spectra in (D) and (E). Blue histogram: SERS probe with GSH. Red histogram: SERS probe in the presence of GSH and other interferences.

provided higher selectivity or response towards GSH than AA. Using a similar strategy, the Cys in Fig. S9† also showed a weaker response to the nanoprobe in comparison with that of GSH.^{29,30} Therefore, this nanoprobe, together with the unique properties of Au–Ag NBs, could provide a strong response towards GSH and then offer the prospect for real-time monitoring GSH in living cells or biofluids.

Conclusions

We demonstrated a SERS nanoprobe for GSH detection with high sensitivity and selectivity. By modifying the metal coordination Nc-Cu^{II} on Au–Ag bimetal NBs, SERS activity and the GSH response were assembled into the Au–Ag NBs/Nc-Cu^{II} nanoprobe. The alteration of SERS spectra resulted from the transformation of Nc-Cu^{II} to Nc-Cu^I in the presence of GSH based on a classical redox reaction, thereby making the nanoprobe suitable for sensitive and selective detection of GSH. This proposed SERS nanoprobe shows great potential for studying and detecting diseases or physiological processes involving GSH.

Conflicts of interest

There are no conflicts to declare.

Acknowledgements

This work was supported by the National Major Scientific and Technological Special Project for “Significant new drugs devel-

opment” (2018ZX09J18112), National Science Foundation of China (21571180, 21505138, 61605221) and Sci-tech Police Project of Anhui Province (1804d08020308).

Notes and references

- S. Bouchet, M. Goni-Urriza, M. Monperrus, R. Guyoneaud, P. Fernandez, C. Heredia, E. Tessier, C. Gassie, D. Point, S. Guedron, D. Acha and D. Amouroux, *Environ. Sci. Technol.*, 2018, **52**, 9758–9767.
- I. Gulcin, P. Taslimi, A. Aygun, N. Sadeghian, E. Bastem, O. I. Kufrevioglu, F. Turkan and F. Sen, *Int. J. Biol. Macromol.*, 2018, **119**, 741–746.
- F. Gong, L. Cheng, N. L. Yang, Q. T. Jin, L. L. Tian, M. Y. Wang, Y. G. Li and Z. Liu, *Nano Lett.*, 2018, **18**, 6037–6044.
- M. H. Sheikh-Mohamadi, N. Etemadi, M. M. Arab, M. Aalifar and M. Arab, *Sci. Hortic.*, 2018, **242**, 195–206.
- F. S. M. Tekie, M. Soleimani, A. Zakerian, M. Dinarvand, M. Amini, R. Dinarvand, E. Arefian and F. Atyabi, *Carbohydr. Polym.*, 2018, **201**, 131–140.
- S. N. Chang, J. M. Lee, H. Oh, U. Kim, B. Ryu and J. H. Park, *Oncol. Lett.*, 2018, **16**, 5482–5488.
- E. J. Shin, Y. G. Hwang, D. T. Pham, J. W. Lee, Y. J. Lee, D. Pyo, X. G. Lei, J. H. Jeong and H. C. Kim, *Neurochem. Int.*, 2018, **118**, 152–165.
- E. J. Shin, Y. G. Hwang, D. T. Pham, J. W. Lee, Y. J. Lee, D. Pyo, J. H. Jeong, X. G. Lei and H. C. Kim, *Environ. Toxicol.*, 2018, **33**, 1019–1028.
- T. Y. Du, H. Zhang, J. Ruan, H. Jiang, H. Y. Chen and X. M. Wang, *ACS Appl. Mater. Interfaces*, 2018, **10**, 12417–12423.
- D. Fan, C. Shang, W. Gu, E. Wang and S. Dong, *ACS Appl. Mater. Interfaces*, 2017, **9**, 25870–25877.
- A. Gil, A. van der Pol, P. van der Meer and R. Bischoff, *J. Pharm. Biomed. Anal.*, 2018, **160**, 289–296.
- B. Bayram, G. Runbach, J. Frank and T. Esatbeyoglu, *J. Agric. Food Chem.*, 2014, **62**, 402–408.
- K. Chen, X. Y. Zhang and D. R. MacFarlane, *Chem. Commun.*, 2017, **53**, 7949–7952.
- X. Y. Li, F. Y. Feng, Z. T. Wu, Y. Z. Liu, X. D. Zhou and J. M. Hu, *Chem. Commun.*, 2017, **53**, 11909–11912.
- H. J. Zhuang, Z. Wang, X. C. Zhang, J. A. Hutchison, W. F. Zhu, Z. Y. Yao, Y. L. Zhao and M. Li, *Chem. Commun.*, 2017, **53**, 1797–1800.
- C. Zong, M. X. Xu, L. J. Xu, T. Wei, X. Ma, X. S. Zheng, R. Hu and B. Ren, *Chem. Rev.*, 2018, **118**, 4946–4980.
- Q. R. Xiong, C. Y. Lim, J. H. Ren, J. J. Zhou, K. Y. Pu, M. B. Chan-Park, H. Mao, Y. C. Lam and H. W. Duan, *Nat. Commun.*, 2018, **9**, 1743.
- S. Q. Xu, B. Y. Wen, L. N. Zhang, H. Zhang, Y. Gao, B. Nataraju, L. P. Xu, X. Wang, J. F. Li and Z. Q. Tian, *Chem. Commun.*, 2018, **54**, 10882–10885.

- 19 J. K. Sahoo, N. M. S. Sirimuthu, A. Canning, M. Zelzer, D. Graham and R. V. Uljin, *Chem. Commun.*, 2016, **52**, 4698–4701.
- 20 Á. Sánchez-Illana, F. Mayr, D. Cuesta-García, J. D. Piñeiro-Ramos, A. Cantarero, M. d. l. Guardia, M. Vento, B. Lendl, G. Quintás and J. Kuligowski, *Anal. Chem.*, 2018, **90**, 9093–9100.
- 21 A. Saha and N. R. Jana, *Anal. Chem.*, 2013, **85**, 9221–9228.
- 22 C. H. Wei, X. Liu, Y. Gao, Y. P. Wu, X. Y. Guo, Y. Ying, Y. Wen and H. F. Yang, *Anal. Chem.*, 2018, **90**, 11333–11339.
- 23 Y. Bu, G. Zhu, S. Li, R. Qi, G. Bhavé, D. Zhang, R. Han, D. Sun, X. Liu, Z. Hu and X. Liu, *ACS Appl. Nano Mater.*, 2018, **1**, 410–417.
- 24 M. H. Kim, X. M. Lu, B. Wiley, E. P. Lee and Y. N. Xia, *J. Phys. Chem. C*, 2008, **112**, 7872–7876.
- 25 S. Y. Ding, J. Yi, J. F. Li, B. Ren, D. Y. Wu, R. Panneerselvam and Z. Q. Tian, *Nat. Rev. Mater.*, 2016, **1**, 1–16.
- 26 M. K. Eggleston, D. R. McMillin, K. S. Koenig and A. J. Pallenberg, *Inorg. Chem.*, 1997, **36**, 172–176.
- 27 J. McCall, D. Bruce, S. Workman, C. Cole and M. M. Richter, *Anal. Chem.*, 2001, **73**, 4617–4620.
- 28 A. N. Tufan, S. Baki, K. Guclu, M. Ozyurek and R. Apak, *J. Agric. Food Chem.*, 2014, **62**, 7111–7117.
- 29 R. Apak, K. Güçlü, M. Özyürek and S. E. Karademir, *J. Agric. Food Chem.*, 2004, **52**, 7970–7981.
- 30 Y. L. Ying, Y. X. Hu, R. Gao, R. J. Yu, Z. Gu, L. P. Lee and Y. T. Long, *J. Am. Chem. Soc.*, 2018, **140**, 5385–5392.